

## Hydrostatic Pressure Dependence of the Paramagnetic Resonance of an S-State Ion in a Noncubic Lattice: $Mn^{2+}$ in Calcite\*†

DAVID F. WAIT

*Harrison M. Randall Laboratory, University of Michigan, Ann Arbor, Michigan*

(Received 16 May 1963; revised manuscript received 28 June 1963)

The interaction of the substitutional impurity ion,  $Mn^{2+}$ , with the crystalline lattice of calcite ( $CaCO_3$ ) was studied at room temperature by means of electron paramagnetic resonance (EPR) at 9.4 kMc/sec as a function of hydrostatic pressure up to 7000 atm. Using a point-charge model, and assuming the parameter  $D$  of the spin Hamiltonian is linearly dependent on the axial crystalline field, it was deduced that the local compressibility about the  $Mn^{2+}$  was equal to the pure host lattice within 30%. The cubic-field parameters  $a_0$  and  $a_0b$  of the spin Hamiltonian depend approximately on the second power of the related crystalline field. Arguments are presented suggesting the point-charge model adequately represents the crystalline field effects, even in the case of covalent bonding, for determining small relative changes in the spin-Hamiltonian parameters. No pressure dependence in the  $g$  factor or linewidth was found. The fractional change in the magnitude of the hyperfine constant was about one-half the fractional change in the volume of the crystal.

### I. INTRODUCTION

THE hydrostatic-pressure dependence of the electron paramagnetic-resonance (EPR) spectrum of a manganous-impurity ion in a calcite ( $CaCO_3$ ) lattice at room temperature was investigated. The motivation was to obtain a better understanding of ionic solid systems with substitutional iron-group impurities. The EPR spectrometer, operated near 9.4 kMc/sec, induced energy transitions between the magnetic sublevels of manganous-ion electrons. The observed spectra were interpreted assuming a Stark splitting of the  ${}^6S_{5/2}$  ground state of a free  $Mn^{2+}$  ion due to an electrostatic field provided by the surrounding calcite lattice. The lattice could be varied by the application of hydrostatic pressures from one to 7000 atm.

This study differs from previous pressure experiments of the EPR spectra of S-state paramagnetic impurities in a diamagnetic host lattice<sup>1</sup> in that the manganese impurity site in calcite has less than cubic symmetry, namely,  $\bar{3}$  symmetry. As a result, additional information is obtained to answer questions concerning the comparison of relative changes in crystalline field with relative compressibility of the sample.

How meaningful it is to assume that the relative change in the spin-Hamiltonian parameters depend only on the relative change in the crystalline electric field is difficult to say. It would be helpful to experimentally determine the  $Dq$  parameter.<sup>2</sup> This also takes into account the radial distributions of the electron density as well as the strength of the electrostatic field. As pointed out, for example, by Kondo,<sup>3</sup> one should also consider the effect of the overlap of the magnetic electrons with

neighboring atoms, and consider the covalency of magnetic electrons with neighboring atoms. Nevertheless, the simplicity of calculating the change in the electrostatic field and the qualified success of electrostatic models for a variety of problems<sup>2,4-7</sup> indicates that this type of analysis for this experiment is realistic.

The relative changes in the microwave spectra due only to changes in the electrostatic field which is expected as the crystal is compressed hydrostatically are indicated in Sec. II. The experimental equipment and experimental technique used are discussed in Sec. III. The experimental results are noted in Sec. IV. A discussion of these results is given in Sec. V.

### II. THEORY

#### Spin Hamiltonian

The unit cell of calcite is shown with the cleavage rhombohedron in Fig. 1. The manganese-ion substitutes for calcium which has two inequivalent sites. Details of the inequivalent carbonate groups are shown in Fig. 2. The electron paramagnetic resonance spectrum of  $Mn^{2+}$  in calcite was first examined in detail by Hurd, Sachs, and Hershberger.<sup>8</sup>

The  $Mn^{2+}$  spectrum may be analyzed in terms of the spin Hamiltonian with parameters consistent with Kikuchi and Matarrese.<sup>9</sup>

$$\begin{aligned} \mathcal{H}_{\text{spin}} = & \beta g_{11} H_z S_z + \frac{1}{2} \beta g_{\perp} (H_+ S_- + H_- S_+) \\ & + A I_z S_z + \frac{1}{2} B (I_+ S_- + I_- S_+) + D S_{20} \\ & + a_0 S_{40} + a_0 b_3 S_{43} - a_0 b_3^* S_{4-3}. \end{aligned} \quad (1)$$

<sup>4</sup> W. Moffitt and C. J. Ballhausen, *Ann. Rev. Phys. Chem.* **7**, 107 (1956).

<sup>5</sup> W. Low, in *Solid State Physics*, edited by F. Seitz and D. Turnbull (Academic Press Inc., New York, 1960), Suppl. 2.

<sup>6</sup> B. Bleaney and K. W. H. Stevens, *Rept. Progr. Phys.* **16**, 108 (1953).

<sup>7</sup> K. D. Bowers and J. Owens, *Rept. Progr. Phys.* **18**, 304 (1955).

<sup>8</sup> F. K. Hurd, M. Sachs, and W. D. Hershberger, *Phys. Rev.* **93**, 373 (1954).

<sup>9</sup> C. Kikuchi and L. M. Matarrese, *J. Chem. Phys.* **33**, 601 (1960).

\* Supported in part by the U. S. Atomic Energy Commission.

† Based on a thesis presented to the Department of Physics, University of Michigan, 1962 in partial fulfillment of the requirements for the degree of Doctor of Philosophy.

<sup>1</sup> W. M. Walsh, Jr., *Phys. Rev.* **122**, 762 (1961); *Phys. Rev. Letters* **4**, 507 (1960).

<sup>2</sup> D. S. McClure, in *Solid State Physics*, edited by F. Seitz and D. Turnbull (Academic Press Inc., New York, 1959), Vol. 9, p. 400.

<sup>3</sup> J. Kondo, *Progr. Theoret. Phys. (Kyoto)* **28**, 1026 (1962).

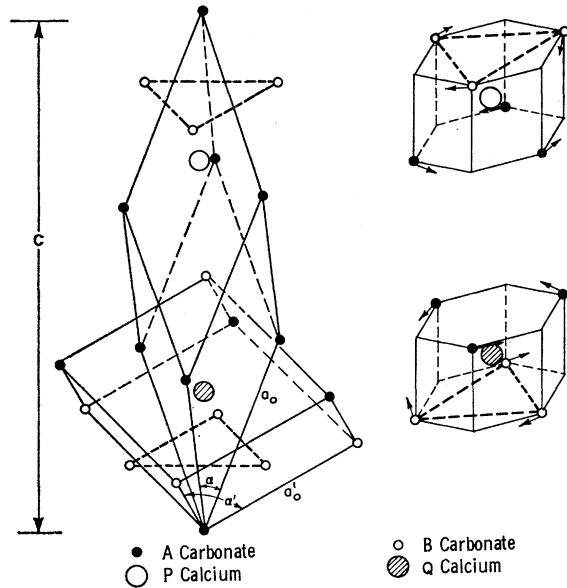


FIG. 1. Unit cell with cleavage rhombohedron and inequivalent hexagonal calcium-site cells.

For convenience, the linear combinations of spin operators which transform under spatial rotation as one of the various spherical harmonics<sup>10</sup> are abbreviated:

$$S_{20} = \frac{1}{3}(3S_z^2 - S^2),$$

$$S_{40} = - (1/180)(35S_z^4 - 30S_z^2S^2 + 25S_z^2 - 6S^2 + 3S^4),$$

$$S_{4\pm 3} = [(35)^{1/2}/(180)]S_{\pm 3}(2S_z \pm 3).$$

In this notation,  $S_{20}$  transforms under rotations as the spherical harmonic  $Y_{20}(\theta, \phi)$ , where the  $z$  axis is along the high-symmetry axis of the crystal, the  $c$  axis, etc. The spin Hamiltonian is appropriate if (1) the low-lying electron states arise from free-ion states of a common multiplet of the orbital quantum number  $L$ , (2) the electron states from different multiplets are separated in energy from the low-lying states by an amount large compared to the perturbation due to the crystalline field, and (3) the perturbation due to the crystalline field is large compared to the free-ion structure, that is, the spin-orbit interaction. The notation used in this Hamiltonian is compared with that used by other authors in an Appendix.

TABLE I. Nonzero, diagonal matrix elements of  $S_{im}'$  for  $S = \frac{5}{2}$ .

$\langle \pm 5/2   S_{20}   \pm 5/2 \rangle = 10/3$
$\langle \pm 3/2   S_{20}   \pm 3/2 \rangle = -2/3$
$\langle \pm 1/2   S_{20}   \pm 1/2 \rangle = -8/3$
$\langle \pm 5/2   S_{40}   \pm 5/2 \rangle = -1/3$
$\langle \pm 3/2   S_{40}   \pm 3/2 \rangle = 1$
$\langle \pm 1/2   S_{40}   \pm 1/2 \rangle = -2/3$

<sup>10</sup>The spherical harmonics are used as defined by A. R. Edmonds, *Angular Momentum in Quantum Mechanics* (Princeton University Press, Princeton, 1957).

TABLE II. Lattice constants for calcite.<sup>a</sup>

Unit cell
$c = 17.020 \text{ \AA}$
$a_0 = 6.361 \text{ \AA}$
$\alpha = 46^\circ 6'$
Cleavage rhombohedron
$a_0' = 6.412 \text{ \AA}$
$\alpha' = 101^\circ 55'$

<sup>a</sup>R. W. C. Wyckoff, *Crystal Structures Handbook* (Interscience Publishers, Inc., New York, 1958).

### Energy Levels

The approximate wave functions are taken to be the free-ion wave functions specified by the quantum numbers  $S = \frac{5}{2}$ ,  $m_S$ ,  $I = \frac{5}{2}$ , and  $m_I$ . The axis of quantization is taken along the applied magnetic field. To first order, the eigenfunctions of the spin Hamiltonian of Eq. (1) may be written as

$$E_{m_S m_I} = g\mu_B m_S + A m_I m_S + D \langle m_S | S_{20} | m_S \rangle + a_0 \langle m_S | S_{40} | m_S \rangle + a_0 b_3 \langle m_S | S_{43} | m_S \rangle - a_0 b_3^* \langle m_S | S_{4-3} | m_S \rangle. \quad (2)$$

The parameters  $g_{II}$  and  $g_I$  are experimentally nearly equal and, therefore, each was set equal to  $g$ . If the applied magnetic field is along the trigonal axis ( $c$  axis) of the crystal, the nonzero matrix elements are given in Table I. In this orientation the matrix elements accompanying  $a_0 b_3$  and  $a_0 b_3^*$  vanish. In order to evaluate these coefficients the high-symmetry axis of the crystal was orientated  $70.0^\circ$  away from the magnetic-field

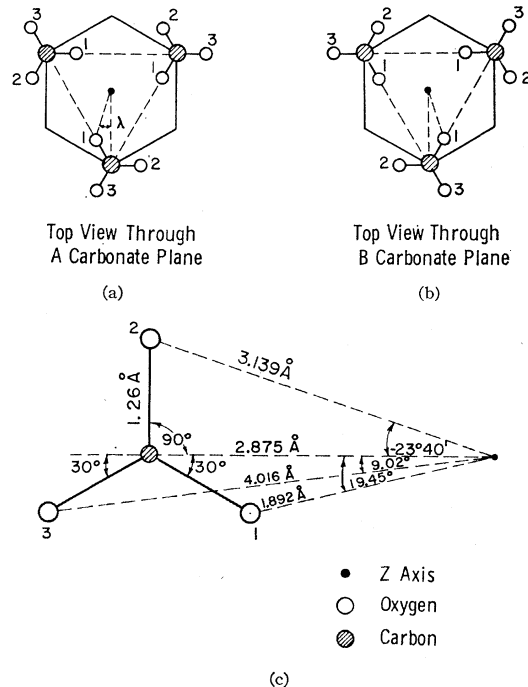


FIG. 2. Details of carbonate groups.

direction. The matrix elements given in Table I may be used when the applied magnetic field is not along the trigonal axis by transforming to a coordinate system whose  $z$  axis is along the applied magnetic field. In this new coordinate system, each of the spin operators  $S_{lm}$  is replaced by a linear combination of spin operators  $S'_{lm}$ . In particular, if the new coordinate system ( $z$  axis is along the magnetic field) is related to the old coordinate system ( $z$  axis is along the trigonal axis of the crystal) by three consecutive rotations from the crystal oriented system through the Euler angles in the order, (1) rotation by  $\alpha$  about the  $z$  axis, (2) rotation by  $\beta$  about the new  $y$  axis, (3) rotation by  $\gamma$  about the newest  $z$  axis, then the appropriate linear combination is<sup>11</sup>:

$$S_{lm}(\theta, \phi) = \sum_{m'=-l}^l \gamma_{mm'}(\alpha, \beta, \gamma) S'_{lm'}(\theta', \phi').$$

For  $m'$  equal zero,<sup>11</sup>

$$\gamma_{m0}(\alpha, \beta, \gamma) = (-1)^m [(4\pi)/(2l+1)]^{1/2} Y_{lm}(\beta, \alpha).$$

Table I contains the appropriate diagonal matrix elements for the  $S_{lm}$  spin operators.

The inequivalent manganous ions differ from each other by a mirror reflection which contains the  $c$  axis of the crystal and passes through a carbon atom. The imaginary part of  $a_0b_3$  denoted  $a_0b$  may be evaluated from the separation in energy of the corresponding transitions for the inequivalent manganous ions.<sup>9</sup>

Contributions to the eigenfunctions due to electric fields with  $Y_{40}(\theta, \phi)$  and  $Y_{43}(\theta, \phi)$  angular dependence are independent of the field contributions with  $Y_{20}(\theta, \phi)$  angular dependence. Although this is evident in the first-order terms of the spin Hamiltonian in Eq. (2), it is true in general, independent of the relative amplitudes of the various multipole contributions. This follows from the fact that eigenfunctions belonging to a particular energy level in calcite must transform according to the irreducible representations of the group  $\bar{3}$ , the site symmetry in calcite.<sup>12</sup> The contribution to the Hamiltonian by the electric field with  $Y_{20}(\theta, \phi)$  symmetry may be split off from the rest of the Hamiltonian. This split-off term transforms as the identity representation of the group  $\bar{3}$ . As the remainder of the Hamiltonian must also transform as the identity representation of  $\bar{3}$ , there can be no off-diagonal matrix elements which

TABLE III. Elastic constants for calcite<sup>a</sup> in units of  $10^{-12}$  (dyn/cm<sup>2</sup>)<sup>-1</sup>.

$s_{11} = 1.10$	$s_{12} = -0.34$
$s_{33} = 1.73$	$s_{13} = -0.43$
$s_{44} = 3.94$	$s_{14} = 0.86$

<sup>a</sup> H. B. Huntington, in *Solid State Physics*, edited by F. Seitz and D. Turnbull (Academic Press Inc., New York, 1958), Vol. 7, p. 282.

<sup>11</sup> See Edmonds (Ref. 10), pp. 54-59.

<sup>12</sup> V. Heine, *Group Theory in Quantum Mechanics* (Pergamon Press, Inc., New York, 1960), p. 42.

TABLE IV. Derived relative crystal-field shifts per 1000-atm hydrostatic pressure.

Model No.	Compression type	(Units of $10^{-6}$ atm <sup>-1</sup> )			
		C-O bond	$\Delta a_{20}/a_{20}$	$\Delta a_{40}/a_{40}$	$\Delta \beta_{43}/\beta_{43}$
1	calcite	constant	-0.50	3.2	4.0
2	calcite	proportional	-2.3	1.5	4.3
3	conformal	proportional	1.5	2.5	2.5
4	uniform	constant	4.3	3.5	4.0

connect the split off part of the Hamiltonian with the remainder of the Hamiltonian. A similar argument holds for contributions to the Hamiltonian of  $Y_{40}(\theta, \phi)$  and  $Y_{43}(\theta, \phi)$  symmetry.

### Models for Relative Changes in Electrostatic Field versus Pressure

In a region which satisfies Laplace's equation, the electric potential due to the electric field may be expressed in the form of a multipole expansion:

$$V(r, \theta, \phi) = \sum_{l,m} a_{lm} r^l Y_{lm}(\theta, \phi). \quad (3)$$

For a point-charge lattice, the coefficients of the expansion (in mks units) are

$$a_{lm} = \{e/[\epsilon(2l+1)]\} \sum Z_i R_i^{-(l+1)} Y_{lm}^*(\Theta_i, \Phi_i), \quad (4)$$

where the summation is over all charges; the  $i$ th charge of magnitude  $eZ_i$  with coordinates  $R_i$ ,  $\Theta_i$ ,  $\Phi_i$ . The symbol  $\epsilon$  denotes the permittivity, is equal to  $8.854 \times 10^{-12}$  F/m. The correspondence between the spin-Hamiltonian coefficients [Eq. (1)] and the crystalline field moments [Eq. (2)] is not yet well understood for  $S$ -state ions. Recent theoretical attempts to relate these parameters have been published by Watanabe<sup>13</sup> and Gabriel, Johnston, and Powell.<sup>14</sup> One purpose of this experiment is to provide information regarding this relationship.

Using Eq. (4), the lattice constants, and the elastic constants shown in Tables II and III, the change in the electrostatic field as a function of pressure was calculated assuming: (1) The electrostatic field is adequately represented by a point-charge lattice, (2) the local compressibility about an impurity ion is the same as if the site were occupied by the usual calcium ion, and (3) the carbon-oxygen bond length of the calcite ion remains unchanged during the compression due to the applied hydrostatic pressure. The results of this calculation<sup>15</sup> are denoted as model No. 1 in Table IV. In order to gain an idea of the restrictiveness of this calculation, several contrasting models were evaluated. For model

<sup>13</sup> H. Watanabe, *Progr. Theoret. Phys. (Kyoto)* **18**, 405 (1957).

<sup>14</sup> J. R. Gabriel, D. F. Johnston, and M. J. D. Powell, *Proc. Roy. Soc. (London)* **A264**, 503 (1961).

<sup>15</sup> Details of this calculation are given in the author's thesis which is available from University Microfilms Inc., Ann Arbor, Michigan.

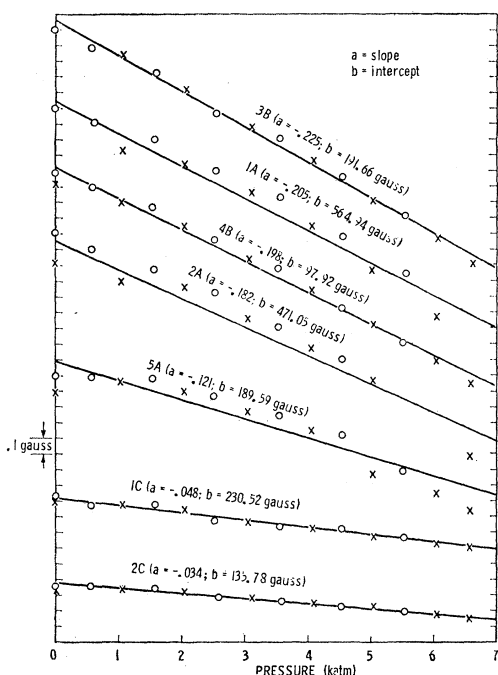


FIG. 3. Pressure shifts of the EPR lines.

No. 2 the carbon-oxygen bonds were assumed to decrease proportionately as the lattice is compressed. For model No. 3, the lattice is assumed to collapse in such a way that the relative shortening along the  $c$  axis and along directions perpendicular to the  $c$  axis are equal. (The elastic constants for calcite indicate a relative shortening along the  $c$  axis 2.7 times as great as the perpendicular direction.) Also the carbon-oxygen bonds in model No. 3 were assumed to decrease proportionately as the lattice. Thus, all internal atomic angles in the solid would be preserved during the compression so that one could say the compression is conformal. The bulk compressibility used for this model is the bulk compressibility of calcite. Model No. 4 is similar to model No. 3 except the carbon-oxygen bond remains constant during compression. The results for these various models are shown in Table IV.

### III. EXPERIMENTAL TECHNIQUES

If the klystron frequency and the magnetic field are measured for the EPR condition for each pressure, and if the magnetic-field dependence of the resonance line is known as a function of klystron frequency, then the shift of the resonance line due to pressure alone can be deduced. Because the pressure shifts are of the order of 1 G out of 3000 G, the klystron frequency, and the magnetic field must be measured to an accuracy somewhat higher than this relative precision. This was accomplished by simultaneously measuring the magnetic field using a proton probe, and measuring the klystron frequency relative to a crystal frequency standard of an electronic counter.

TABLE V. Energy-transition notation.

Transition	Initial level		Final level	
	$m_s$	$m_I$	$m_s$	$m_I$
1A	$-\frac{5}{2}$	$-\frac{5}{2}$	$-\frac{3}{2}$	$-\frac{5}{2}$
1C	$-\frac{1}{2}$	$-\frac{5}{2}$	$\frac{1}{2}$	$-\frac{5}{2}$
2A	$-\frac{5}{2}$	$-\frac{3}{2}$	$-\frac{3}{2}$	$-\frac{3}{2}$
2C	$-\frac{1}{2}$	$-\frac{3}{2}$	$\frac{1}{2}$	$-\frac{3}{2}$
3B	$-\frac{3}{2}$	$-\frac{1}{2}$	$-\frac{1}{2}$	$-\frac{1}{2}$
4B	$-\frac{3}{2}$	$\frac{1}{2}$	$\frac{1}{2}$	$\frac{1}{2}$
5A	$-\frac{5}{2}$	$\frac{3}{2}$	$-\frac{3}{2}$	$\frac{3}{2}$

The magnetic field was generated by a Varian 12-in. magnet with 3-in. pole cap separation (Model V-4012-3B). The EPR sample and the proton-probe sample were placed symmetrically in the median plane of the magnet about the magnetic center. Thus, the EPR sample and proton-probe sample should always be close to the same magnetic-field contour-independent in first order to the hysteresis properties of the magnet iron. A shift as small as  $\pm 0.02$  G could be determined by measuring the proton resonant frequency with a crystal-controlled electronic counter (Hewlett-Packard Model 524B). The klystron frequency was measured by means of a Hewlett-Packard Model 540A transfer oscillator and the same electronic counter.

The EPR spectrometer employs a direct crystal detection system (using Varian V153C/6315 300 mW klystron and Microwave Associates 1N23E crystal) of conventional design.<sup>16</sup> Hydrostatic pressures were generated and measured using a Harwood Engineering A 2.5J intensifier and related equipment.<sup>17</sup> The high-pressure seals were patterned after Walsh.<sup>18</sup> To eliminate an inconvenient capacitive coupling in Walsh's high-pressure microwave cavity design, and to reduce the portion of the coaxial cavity under pressure, the pressure sealing cone was made part of an electrically continuous center conductor of the coaxial cavity. Thus, only the sample end of the cavity is under pressure. The entrance of the cavity (the electrical discontinuity at the coaxial guide to waveguide conversion) is now accessible to adjust the tuning of the cavity while the sample is under pressure. This is desirable since the resonant characteristics of the cavity are modified as the pressure in the sample end is changed. The coupling into the microwave cavity is varied by means of a below cutoff attenuator as described by Gordon<sup>19</sup> placed near the coaxial guide to rectangular wave-guide converter. Because the pressure seal is within the resonant structure,<sup>20</sup> a second sample can simultaneously be positioned in the room pressure portion of the cavity. The cavity was eight wavelengths

<sup>16</sup> G. Feher, Bell System Tech. J. **36**, 449 (1957).

<sup>17</sup> Harwood Engineering Company, Walpole, Massachusetts.

<sup>18</sup> W. M. Walsh, Jr., and N. Bloembergen, Phys. Rev. **107**, 904 (1957).

<sup>19</sup> J. P. Gordon, Rev. Sci. Instr. **32**, 658 (1961).

<sup>20</sup> A detailed analysis and construction details of the cavity are being prepared for publication.

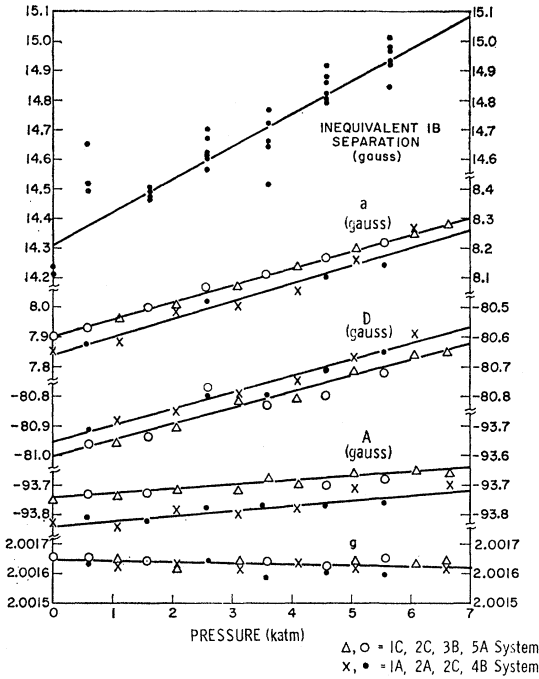


Fig. 4. Pressure shifts of spin-Hamiltonian parameters.

long at 9.42 kMc/sec. The length of the cavity was in anticipation of the two sample experiments for which the instrumentation is now being completed. At the resonant frequency of 9.42 kMc/sec, the cavity  $Q$  is approximately 150. The resonant frequency decreased about 0.0025 kMc/sec for each 1000-atm pressure.

#### IV. RESULTS

There are thirty  $\Delta m_S = \pm 1$ ,  $\Delta m_I = 0$  transitions among the  $(2S+1)(2I+1)$  energy levels of  $Mn^{2+}$ , or 36 energy levels since  $S = \frac{5}{2}$  and  $I = \frac{5}{2}$ . Of the 30 transitions, 14 are nonoverlapping lines when the magnetic field is along the crystalline axis, and the klystron frequency is 9.4 kMc/sec. The pressure dependence of each of these clear lines was determined. More detailed data were taken on seven of the 14 lines. The pressure dependence of the seven lines are shown in Fig. 3. The transitions used, and their dependence on the spin-Hamiltonian parameters are shown in Tables V and VI. The pressure dependence of the spin-Hamiltonian parameters  $a_0$ ,  $D$ ,  $A$ , and  $g$  using the pressure dependence of these seven

 TABLE VI. Transition energies for  $\beta = 0^\circ$  (first order).

$h\nu_{1A} = g\mu_B H_{1A} - \frac{5}{2}A - 4D + \frac{3}{2}a$
$h\nu_{1C} = g\mu_B H_{1C} - \frac{5}{2}A$
$h\nu_{2A} = g\mu_B H_{2A} - \frac{3}{2}A - 4D + \frac{3}{2}a$
$h\nu_{2C} = g\mu_B H_{2C} - \frac{3}{2}A$
$h\nu_{3B} = g\mu_B H_{3B} - \frac{1}{2}A - 2D - (5/3)a$
$h\nu_{4B} = g\mu_B H_{4B} + \frac{1}{2}A - 2D - (5/3)a$
$h\nu_{5A} = g\mu_B H_{5A} + \frac{3}{2}A - 4D + \frac{3}{2}a$

 TABLE VII. Experimental pressure shifts of the spin-Hamiltonian parameters in units of  $10^{-6} \text{ atm}^{-1}$ .

$\Delta g/g = 0.004 \pm 0.016$
$\Delta A/A = -0.17 \pm 0.05$
$\Delta D/D = -0.66 \pm 0.06$
$\Delta a/a = 7.6 \pm 0.7$
$\Delta ab/ab = 7.7 \pm 0.4$

lines is shown in Fig. 4. Also shown in Fig. 4 is the separation in gauss between the inequivalent  $1B$  (Table V) transitions when the crystal is oriented at  $\beta = 70.0^\circ$ ,  $\alpha = 16.2^\circ$ . From the pressure dependence of this separation, the pressure dependence of  $a_0b$  is determined. The difference in energy for the inequivalent  $1B$  transition is,<sup>21</sup>

$$h\nu_{1B}^{(P)} - h\nu_{1B}^{(Q)} = - (5/3)(35)^{1/2} a_0 b \cos \beta \sin^3 \beta \sin 3\alpha.$$

The fact that two least-square-fit lines are shown for several of the parameters in Fig. 4 is because the off-diagonal matrix elements of the terms  $a_0 b_3 S_{43} - a_0 b_3^* S_{4-3}$  were neglected. The slopes of the spin-Hamiltonian parameters as deduced from Fig. 3 are listed in Table VII. The error indicated with the slopes is an estimation which includes, besides statistical deviation, estimates of several systematic errors. Systematic errors taken into account are (a) distortion of the line by the electronic detection system, which was estimated as being less than  $\pm 0.02$  G, (b) variations of the modulation pickup, less than  $\pm 0.05$  G, (c) the error introduced by assuming the pressure dependence of the change in the spin Hamiltonian to be linear, less than 3% of the pressure shift, and (d) the error due to the limitation in orienting the crystal, less than 0.6% of the pressure shift.

#### V. CONCLUSIONS

##### Dependence of Zero-Field Splitting on Crystalline Fields

From the fact that the experimental  $\Delta D/D$  is approximately equal to the calculated  $\Delta a_{20}/a_{20}$ , one may conclude that the spin-Hamiltonian parameter  $D$  varies linearly (more precisely  $1.3 \pm 0.2$  power) with the  $Y_{20}(\theta, \phi)$  symmetry component of the electrostatic field. Because  $\Delta a_0/a_0$  is approximately twice  $\Delta a_{40}/a_{40}$  and  $\Delta a_0 b/a_0 b$  is approximately twice  $\Delta \beta_{43}/\beta_{43}$ ,  $a_0$  varies quadratically with the  $Y_{40}(\theta, \phi)$  component of the electrostatic field, and  $a_0 b$  varies quadratically with the  $Y_{43}(\theta, \phi)$  component (more precisely the  $2.4 \pm 0.4$  and  $1.9 \pm 0.3$  power, respectively). This conclusion rests upon several assumptions: (a) that the point-charge model chosen adequately represents the relative changes in the electrostatic field; (b) that the compressibility about an impurity site is the same as if the normal calcium occupied the site; and (c) that the change in

<sup>21</sup> See Kikuchi and Matarrese (Ref. 9). The Euler angles are chosen to agree with Edmonds (Ref. 10).

the spin-Hamiltonian parameter depends only upon the change in the intensity of the electrostatic field.

### Adequacy of the Point-Charge Model

If instead of the point-charge model one were to consider a distributed charge model, then the crystalline field moments noted in Eq. (4) would be replaced by

$$a_{lm} = \frac{1}{\epsilon(2l+1)} \int \frac{Y_{lm}^*(\Theta, \Phi)}{R^{l+1}} \rho(R, \Theta, \Phi) dV,$$

where the integration extends over all charge density  $\rho(R, \Theta, \Phi)$ . For the special case where the charge distribution contracts proportionately such that after compression the new density  $\rho'(R', \Theta', \Phi')$  is related to the original distribution  $\rho(R, \Theta, \Phi)$  by

$$\rho'(R', \Theta', \Phi') = \rho(R + \Delta R, \Theta, \Phi),$$

the new coefficients  $a_{lm}'$  are related to the original  $a_{lm}$  by

$$a_{lm}' = a_{lm} - (l+1)(\Delta R/R)a_{lm}.$$

The term  $\Delta R/R$  is a constant independent of  $R$ . Thus, for a conformal (angle preserving), proportional contraction, the relative change of any coefficient of the multipole expansion is known for any arbitrary charge distributions:

$$\Delta a_{lm}/a_{lm} = -(l+1)\Delta R/R.$$

For cubic crystals then, we expect any reasonable model to accurately predict relative changes in the crystalline field providing the electron density compresses proportionally as the crystal compresses. There is reason to hope the point-charge model will do an adequate job for a less symmetric compression such as in calcite. In this regard it is helpful to compare the results of the preferred point-charge model for calcite (model No. 1) with the results of the contrasting models. In particular, the conformal model No. 3 is related to model No. 2 as model No. 4 is related to model No. 1. A comparison suggests that the relative changes in the cubic components of the electric field amplitude denoted by  $a_{40}$  and  $a_{43}$  are not too sensitive to the model chosen. The lower symmetry component of the field whose amplitude is denoted by  $a_{20}$  is more sensitive to the details of the lattice compression. A more difficult test of the point-charge model is represented by the work of Kikuchi and Matarrese<sup>9</sup> who used the point-charge model to predict the parameter  $a_0b$  within<sup>22</sup> 15% using the experimental value of  $a_0$  to eliminate an unknown radial integration.

The carbon-oxygen bond length in the carbonate ion is expected to remain relatively unchanged in length because of the covalent nature of this bond. This is consistent with the experimental results.

<sup>22</sup> By coincidence the results of Kikuchi and Matarrese are not sensitive to the relation assumed between  $a$  and  $a_0b$  to  $a_{40}$  and  $\beta_{43}$ . Kikuchi and Matarrese assumed  $a$  and  $a_0b$  are linearly proportional to  $a_{40}$  and  $\beta_{43}$ . The agreement improves slightly if one assumes a quadratic dependence.

### Compressibility About Impurity Site

The experimental results suggest that the compressibility about the impurity ion is not markedly different than that of the rest of the crystal. That is, the parameter  $D$  is expected to depend linearly<sup>13,23-24</sup> upon the crystalline electric field, and experimentally it is the  $1.3 \pm 0.2$  power.

### Pressure Dependence of $g$ and $A$

Within the experimental error, there was no change in the  $g$  value, or in the linewidths.

The small decrease in magnitude of the hyperfine splitting parameter  $A$  as a function of pressure noted in Fig. 4 might imply that the  $Mn^{2+}$  ion is becoming more covalently bound to the crystal. Using the graph in the paper by Matumura<sup>25</sup> concerning  $Mn^{2+}$  in cubic lattices as a guide, the hyperfine splitting in calcite would suggest the crystal is about 95% ionic. That is, about as ionic as any of the 22 crystals examined by Matumura. Using his slope in the graph of hyperfine constant versus ionicity suggests that for a 1% change in ionicity,  $\Delta A/A = 19 \times 10^{-3}$ . Therefore, the relative change in the hyperfine splitting noted in Fig. 4 suggests that  $Mn^{2+}$  becomes 0.01% more covalently bonded to the calcite lattice for each 1000 atm of pressure.

An alternate mechanism to explain the change in the hyperfine constant was presented by Walsh<sup>1</sup> who suggested that the change in the hyperfine constant versus pressure might be due to an expansion of the  $3d$  wave functions. This suggestion is in accord with a neutron diffraction experiment<sup>26</sup> which indicated that the mean  $d$ -shell electron distribution in a solid is expanded by 10% over the distribution for the free ion for several manganese compounds. If one assumes that a 10% expansion of the wave function reduced  $A_{40}$  from  $100 \times 10^{-4}$  to  $87.82 \times 10^{-4} \text{ cm}^{-1}$ , then the change in  $A$  versus pressure would be accounted for by a 0.014% expansion per 1000-atm pressure applied. That the hyperfine splitting constant  $A$  decreases with increasing  $3d$  orbitals is in accord with the results of the molecular beam experiment of Woodgate and Martin<sup>27</sup> for the  $3d^5 4s^2 6S_{5/2}$  ground state of neutral  $Mn^{55}$ .

### Comparison with Previous Experiments

The cubic-field splitting parameter  $a_0$  for  $Mn^{2+}$  in calcite is 7.63 G and is comparable with 8.53 G for  $Mn^{2+}$  in ZnS. The crystalline electric fields are of opposite signs, however, because  $Mn^{2+}$  in calcite has octahedral coordination to the nearest neighboring ions while  $Mn^{2+}$  in ZnS has tetrahedral coordination. Based on point-

<sup>23</sup> M. H. L. Pryce, Phys. Rev. **80**, 1107 (1950).

<sup>24</sup> S. Geschwind, Phys. Rev. **112**, 363 (1961).

<sup>25</sup> O. Matumura, J. Phys. Soc. Japan **14**, 108 (1959).

<sup>26</sup> J. M. Hastings, N. Elliott, and L. M. Corliss, Phys. Rev. **115**, 13 (1959).

<sup>27</sup> G. K. Woodgate and J. S. Martin, Proc. Phys. Soc. (London) **A70**, 485 (1957).

charge models,  $a_0$  for  $\text{Mn}^{2+}$  depends on the 1.9 power of the cubic field<sup>28</sup> in ZnS and the  $2.4 \pm 0.4$  power of the cubic field in calcite. Although ZnS is not strictly an ionic crystal, this does not necessarily invalidate this comparison, as has been discussed earlier. It is interesting that this agrees with what one might expect on the basis of the early papers by Watanabe.<sup>13,29</sup> That is, the cubic field splitting parameter  $a_0$  for  $\text{Mn}^{2+}$  is in the first approximation, independent of the sign of the cubic crystal field. For  $\text{Mn}^{2+}$  in host lattices in which  $a_0$  is greater, the dependence upon the cubic crystal field is greater.<sup>1</sup>

In conclusion then, the zero-field splitting in calcite depends on the square of the cubic-electrostatic field. This is comparable with the square dependence of  $\text{Mn}^{2+}$  in ZnS which has similar cubic field splittings, but opposite sign. For  $\text{Mn}^{2+}$  in host lattices in which  $a_0$  is greater, the dependence upon the cubic crystal field is greater. This difference in pressure dependence is not in conflict with the work of Gabriel, Johnston, and Powell.<sup>14</sup> However, as this theory depends thus far on unmeasured parameters such as the position of the spin doublets of the free ion spectra as well as on the unmeasured  $Dq$  parameter for  $\text{Mn}^{2+}$  in calcite, a quantitative comparison is not possible. Walsh<sup>1</sup> reported that the pressure dependence of  $\text{Fe}^{3+}$  on the crystalline field of MgO was similar to the  $\text{Mn}^{2+}$  pressure dependence. Based on Gabriel, Johnston, and Powell<sup>14</sup> theory, a  $\text{Fe}^{3+}$  ion in calcite is not necessarily expected to have the same dependence on the cubic crystalline electric field as  $\text{Mn}^{2+}$  ion. It is, therefore, of some interest to examine the pressure dependence of this ion in calcite. This experiment is in progress in this laboratory.

#### ACKNOWLEDGMENTS

It is a pleasure to acknowledge Professor Richard H. Sands for the suggestion of this problem and for his

<sup>28</sup> See Walsh (Ref. 1). Instead of the crystal field parameter  $a_{40}$ , Walsh discusses the problem in terms of the parameter  $Dq$  which includes also a radial integration of the  $3d$  wave function (Ref. 2). From a perturbation approach, the change of the energy levels due to the perturbing Hamiltonian is large compared with the change due to correcting the first-order wave functions. Thus, we assume the power dependence of any of the spin Hamiltonian parameters on  $a_{40}$  or  $Dq$  to be the same.

<sup>29</sup> Hiroshi Watanabe, Phys. Rev. Letters 4, 410 (1960).

advice and assistance. The author would also like to thank H. R. Roemer and A. Wagner of the physics shop for the construction of mechanical equipment; G. I. Geikas for checking the numerical calculations; A. F. Clark, P. A. Franken, K. T. Hecht, C. Kikuchi, S. A. Marshall, L. M. Matarrese, H. Watanabe, and G. Weinreich for many helpful discussions; and the members of the A.E.C. Resonance Group for support, suggestions, and assistance.

#### APPENDIX. SPIN HAMILTONIAN NOTATION

Using the same abbreviations as used for Eq. (1), the corresponding spin Hamiltonian for a cubic crystal ( $z$  axis taken along the threefold axis) would be written as

$$\mathcal{H}_c = g\beta\mathbf{H}\cdot\mathbf{S} + A\mathbf{I}\cdot\mathbf{S} + a[S_{40} + (10/7)^{1/2}(S_{43} - S_{4-3})].$$

For the cubic crystal it is also common to choose the  $z$  axis along the fourfold axis. For this case, the spin Hamiltonian becomes

$$3\mathcal{C}_c = g\beta\mathbf{H}\cdot\mathbf{S} + A\mathbf{I}\cdot\mathbf{S} - \frac{3}{2}a[S_{40} + (5/14)^{1/2}(S_{44} + S_{4-4})],$$

where

$$S_{4\pm 4} = -[(70)^{1/2}/360]S_{\pm 4}^4.$$

Thus, the parameter  $a_0$  of Eq. (1) corresponds to the cubic field-splitting parameter  $a$ .

In terms of the spin-Hamiltonian parameters used by Bleaney and Trenam<sup>30</sup> Eq. (1) would have been written as

$$\mathcal{H}_{\text{spin}} = \beta g_{11}H_z S_z + \frac{1}{2}\beta g_{11}(H_+ S_- + H_- S_+) + DS_{20} + (a_b - F)S_{40} + a_b(10/7)^{1/2}(S_{43} - S_{4-3}).$$

The subscript in the symbol  $a_b$  has been added to distinguish this parameter from the parameter  $a$  for the cubic field.

The parameters  $D'$  and  $d'$  used by Hurd, Sachs, and Hershberger<sup>8</sup> are related in the following way to those used for this paper:

$$D' = \frac{1}{2}D,$$

$$d' = -(1/1440)a_0.$$

<sup>30</sup> B. Bleaney and R. S. Trenam, Proc. Roy. Soc. (London) A223, 1 (1954).